Experimental investigation of tack coat fatigue performance: Towards an improved lifetime assessment of pavement structure interfaces

Malick Diakhaté, Anne Millien, Christophe Petit, Annabelle Phelipot-Mardelé, Bertrand Pouteau

Experimental investigation of tack coat fatigue performance: Towards an improved lifetime assessment of pavement structure interfaces

M. Diakhaté [a], A. Millien [a], C. Petit [a], A. Phelipot-Mardelé [b], B. Pouteau [c]

[a] *Université de Limoges, GEMH-GCD, Bd J. Derche, 19300 Egletons, France*

[b] *Université Européenne de Bretagne, LGCGM, IUT de Rennes, 3 rue du Clos Courtel, BP 90422, 35704 Rennes Cedex, France*

[c] *Eurovia, Centre de Recherche de Mérignac, 22 rue T. Sabine, 33703 Mérignac, France*

Corresponding author: M. Diakhaté – e-mail: malick.diakhate@unilim.fr; Tel: +335 55 93 45 28; Fax: +335 55 93 45 31

Abstract

This paper focuses on investigating the bonding fatigue performance between two asphalt concrete (AC) layers. For purposes of this experimental campaign, a customised double shear testing device was designed. Two interface conditions have been analysed herein: with and without a tack coat. Moreover, the corresponding fatigue behaviour has been analysed at two temperatures: 10°C and 20°C. As expected, the absence of a tack coat leads to a decrease in bonding fatigue performance. Since fatigue tests are highly time-consuming, a method that allows predicting the conventional interface fatigue law from accelerated shear fatigue tests has been proposed. Other novel findings on interface fatigue behaviour will also be discussed. In addition to these fatigue results, an interface failure model is proposed to evaluate the interface lifetime. Incorporating interface fatigue performance into pavement analysis proves to be a key parameter in describing *in situ* pavement conditions and assessing pavement durability.

Keywords: Pavement durability; interface; tack coat; bonding fatigue performance; double shear test; lifetime.

1. Introduction

In the recent past, interface shear performance has been widely investigated [1-13], especially given that the behaviour of in-service pavements has on occasion revealed several types of premature distresses, potentially due to an inadequate selection of interface boundary conditions during the pavement design stage. During the design process, the currently held assumptions of full bonding vs. no friction between adjacent layers in fact fail to address practical realities. The stress distribution in a pavement structure is influenced by the bonding state at each interface [10,11]. Taking into account the interface bonding state in a pavement analysis therefore proves to be of great importance by improving the assessment of pavement lifetime (or residual lifetime).

In particular, if the necessary bonding level is not introduced at the uppermost interface, then the wearing course may become the only layer to withstand traffic loads (since shear continuity will be lacking at the interface); distresses thus appear earlier than expected. In addition, the shear stress level at the uppermost interface increases with rising traffic loads and thinner wearing courses. Field observations have underscored the need to ensure an excellent bond of adjacent layers, notably on road sections where vehicles are more likely to apply horizontal forces, such as small-radius curves, steep ramps and braking/acceleration zones [3,4].

Even though field observations on roads have highlighted the need to understand actual interface behaviour in order to more accurately compute the useful lifetime of pavement structures, the laboratory campaigns carried out were nonetheless restricted to monotonic tests (direct shear, pull-off, wedge-splitting, etc.). Raab *et al*. summarised the test methods and devices for the determination of bond between asphalt pavement layers regarding shear testing [12]. The practice of subjecting a pavement structure under traffic load to a fatigue loading is by no means a new technique, which makes it obvious that loads acting at the interfaces are also cyclic.

To simulate the repetitive load of moving vehicles, Romanoschi and Metcalf [3] proposed a laboratory test configuration to perform shear fatigue tests on asphalt concrete layer interfaces. The specimen is subjected to both a normal and shear load. To include the normal force, the testing device, developed by Romanoschi [4], allowed for the longitudinal axis of the test specimen being at a 25.5° angle with the vertical, so that the shear stress at the interface is half the normal stress. A vertical load is applied with a minimum of 10% of the maximum load and with a frequency of 5 Hz. Fatigue tests on two types of interface (with and without tack coat) were performed at 25°C. Four normal stresses (0.50, 0.75, 1.00, and 1.25) were selected to be within the range of normal stress values encountered at the interfaces of road and airfield pavements. Elastic and permanent displacements at the interface in normal and tangential directions were recorded for each cycle, and the cyclic tests were stopped when the permanent shear displacement (PSD) at the interface reached 6 mm or when it was considered that the number of loading cycles corresponding to a PSD of 6 mm could be extrapolated [3,4,14]. The parameter ND1 (number of loading cycles that leads to an increase of PSD of 1 mm) gives information of the interface bond fatigue performance.

At the Technical University of Dresden (Germany), the development of a dynamic version of the Leutner shear test is under way. The asphalt concrete specimen is subjected to both a shear and normal force [13]. In this cyclic testing on the interface bond, different parameters such as temperature (-10°C, +10°C, +30°C and +50°C), normal stress (0 to 1.11 N/mm^2) and the loading function (sinusoidal function with amplitudes from 0.005 to 0.1 mm and a frequency from 1 to 15 Hz) were included. The purpose of the project was to find an "interlayer bonding factor" which can be used for pavement design in BISAR or in finite element programs.

This paper will present the results from a research project devoted to both the experimental and numerical study of fatigue shear behaviour at interfaces. One objective of this research has been to propose an additional failure criterion in the pavement design method. With most flexible pavement design methods, the structure is assessed on the basis of the tensile fatigue performance of bituminous layers as well as the rutting performance of unbound granular layers. These results will enable the pavement designer to evaluate the lifetimes of both interface bonding and the material layers. Incorporating interface fatigue performance into pavement analysis therefore serves as a key means of providing more accurate results (i.e. description of the *in situ* pavement conditions, pavement lifetime determination).

The interface fatigue performance between two distinct asphalt concrete (AC) layers will be investigated. Two types of interface conditions are analysed herein: with and without an asphalt tack coat. For purposes of this experimental campaign, a specific double shear testing device has also been designed and manufactured [14].

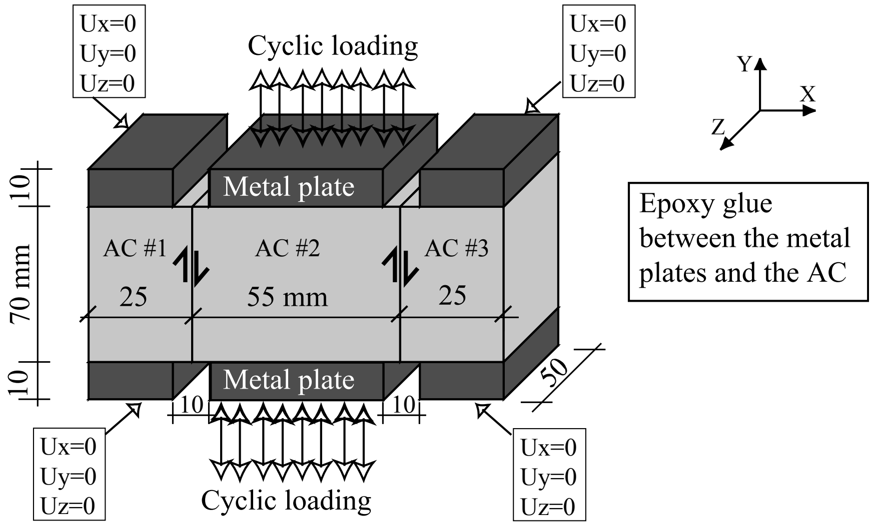

Fig. 1. Schematic diagram of the double shear test

2. Experimental campaign

2.1 Presentation of the testing device

The GEMH-GCD laboratory (*Université de Limoges*, France) has successfully introduced a double shear test, based on the compact shear test, to investigate crack propagation within asphalt concrete under a mode II fatigue loading [15]. In the same laboratory, Diakhaté *et al.* used this double shear device (known as COLAREG) to conduct a feasibility study on the shear fatigue behaviour of tack coats [9].

The double shear test (DST) in the laboratory involves a specimen consisting of three layers bonded two-by-two with the same tack coat. The case of an interface without a tack coat can also be tested using this set-up. The two side layers (AC #1 and AC #3) are fixed during the test, and the central layer (AC #2) is subjected to a load (Fig. 1). To investigate tack coat shear behaviour, the advantage of a double shear test lies in the fact that both interfaces symmetrically undergo a relatively pure shear loading [14].

However, since the COLAREG device used in the previous study [9] does not allow conducting either oligocyclic or monotonic tests beyond fatigue, a more versatile device would need to be designed and built. During an initial stage, the finite element programmes Cast3M and NISA® were used to model the testing device. This study is intended to obtain a relatively pure shear loading at the interfaces by means of optimising both the specimen and device geometries. The second stage involves validating the manufacturing quality of the device (by shear loading at the interfaces) using optical methods [14]. Fig. 2 displays the completed double shear test device.

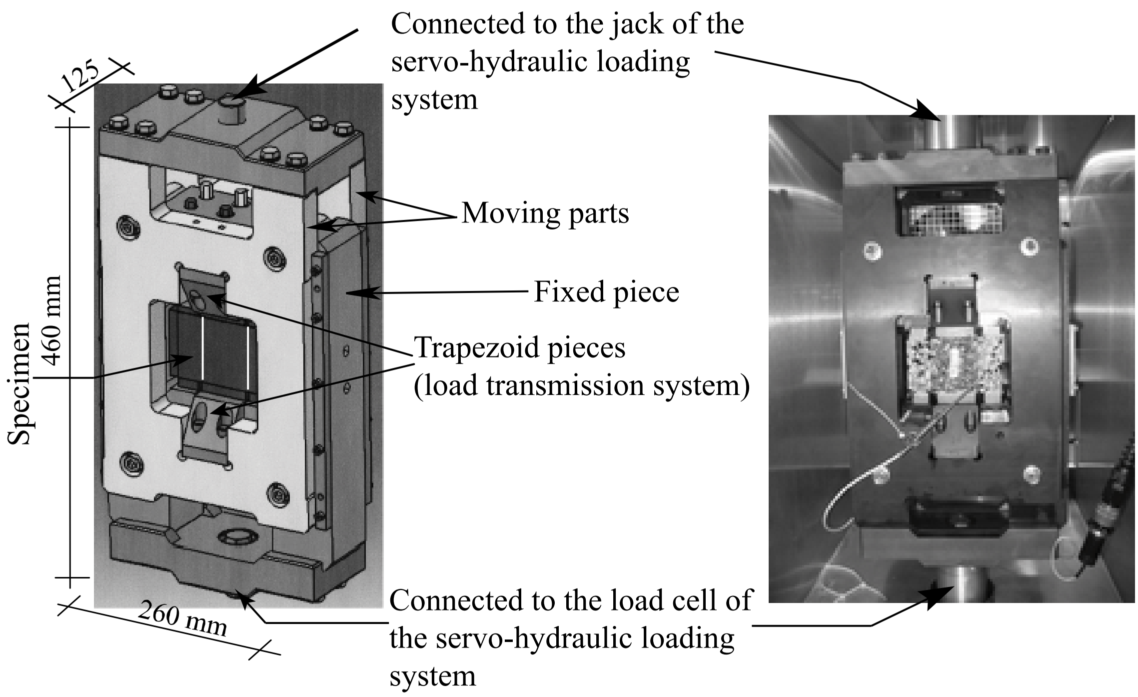

Fig. 2. Schematic presentation and photograph of the double shear test device

2.2 Asphalt concrete and interface conditions

Two types of interfaces are studied as part of this experimental campaign: the first, referred to as TC-70/100, calls for the asphalt concrete layers to be bonded with a tack coat; while the second entails bonding the two layers without a tack coat (WTC). The tack coat used in this campaign is a conventional, rapid-setting cationic emulsion (reference C65B4, according to the European Standard EN 13808:2004(F)); it contains approximately 65% bitumen (pen 70/100).

The two types of asphalt concrete selected for this experiment were manufactured in the laboratory. Both mixes have been formulated with the same pure bitumen (pen 35/50). The design characteristics of these common asphalt concretes are given in Table 1 below.

Table 1. Design characteristics of the tested asphalt concrete (AC) mixes

-	Mix type	Nominal aggregate size	Geological nature	Binder content, mass (%)	Mean thickness (mm)	Air void content (%)
Upper AC layer	Very thin layer	0/10 mm	Grey diorite	5.6	30	12
Lower AC layer	Thick layer	0/10 mm	Pink quartzite sandstone	6.0	50	7

2.3 Production of DST specimens

The double shear test (DST) involves a specimen composed of three asphalt layers. Fig. 3 presents the method employed to obtain the desired specimen shape. The advantage of this method is that both interfaces exhibit the same characteristics, in terms of compaction, roughness, tack coat application rate, etc. Moreover, this method can be applied to field specimens (either slabs or cores).

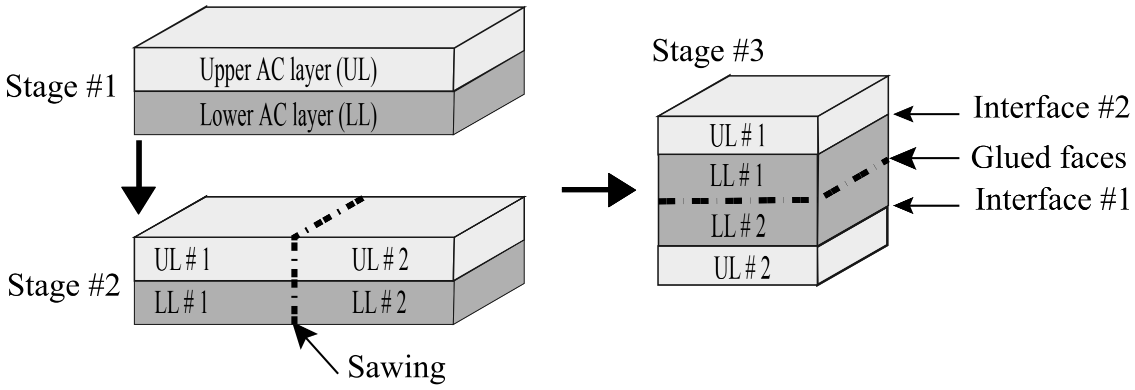

Fig. 3. Fabrication method employed for the three AC-layer specimen

To produce the desired specimen using the method in Fig. 3, the first stage consisted of creating a double-layered slab. After sawing the slab (stage #2), the two resulting parts were glued together (stage #3) with a two-component epoxy glue. Following polymerisation of the glue, a sawing process allowed extracting specimens with the specified geometry (i.e. L x H x W: 105 mm x 70 mm x 50 mm).

In the first stage of the previously presented method, a mould (measuring 600 mm long, 400 mm wide and 80 mm high) was used to prepare the double-layered slab. Once the hot mix asphalt (160°C) had been poured into the mould, the French rolling wheel compactor (Fig. 4) compacted the mixture to a thickness of 50 mm, in accordance with European Standard NF EN 12697-33. After cooling for two hours, the temperature at the upper surface of the layer equalled approx. 40°C and the tack coat was then uniformly applied at a rate of 300 g/m² (residual bitumen). This temperature (40°C) was chosen because the tack coat was stored in a climatic chamber at 60°C. Once the tack coat had been applied, a 2-hour rest time was considered adequate to ensure the corresponding breaking process. Afterwards, the compaction process was repeated in order to produce the upper asphalt concrete layer (30-mm thickness).

(a) Rolling wheel compactor (b) Tack coat application (c) Double-layered slab

Fig. 4. Laboratory manufacturing process for a double-layered slab specimen

After the sawing and gluing stage (#3, Fig. 3), twelve laboratory specimens were obtained by repeating the sawing operation.

To complete the DST specimen fabrication step, a special device was subsequently used to glue steel plates onto the corresponding specimen faces (Fig. 5). A minimum rest time of 1 day was observed to allow for the glue to set. This last stage served to ensure the best alignment of steel plates in relation to the double shear loading configuration, as well as an optimal dimension of the DST specimen in order to maintain its good fit with the DST device. Since AC is a viscoelastic material, 12 screws were used to fasten the plates glued onto the specimen with the DST device.

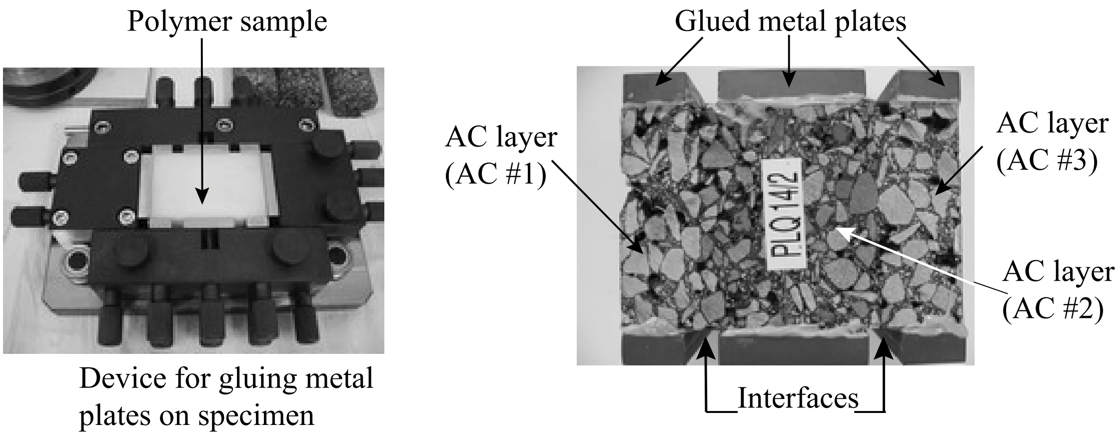

Fig. 5. Special device used for gluing metal plates onto specimen faces

2.4 Experimental programme and loading conditions

As part of this research project devoted to characterising interface shear behaviour, the entire experimental programme included both monotonic and fatigue tests. The analysis presented in this paper however has been restricted to an interpretation of just the shear fatigue test results.

The experimental programme was intended to carry out both oligocyclic and fatigue tests in order to span a number of loading cycles to failure between 10 and several million. A total of 48 cyclic tests were conducted at a frequency of 10 Hz and under force control (given that specimens consisted of thin layers). A symmetric and alternating sinusoidal cycle was applied.

A servo-hydraulic MTS® press was used to apply the shear loading. A load cell (±100 kN) measured both the force values and relative tangential displacement values between the central layer (AC #2) and the two lateral layers (AC #1 and AC #3) of the DST specimen, using an external extensometer (±1 mm) located nearby. During the fatigue test, these values (force and displacement) were recorded with a data acquisition system. In addition to the mechanical loading conditions, two temperatures (10°C and 20°C) were set as test conditions by means of introducing a climatic chamber placed around the double shear device (Fig. 6). Before beginning the test, the temperature was homogenised within the specimen for at least six hours.

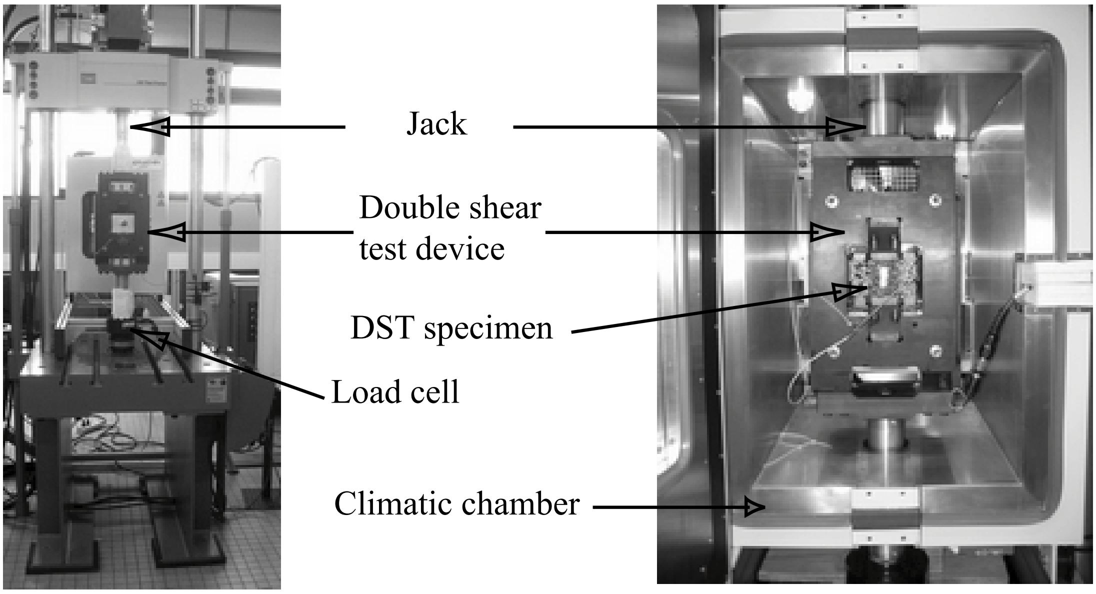

Overall view of the servo-hydraulic frame (MTS)

Climatic chamber around the Double shear test device

Fig. 6. Fatigue testing equipment

Under force control, the cyclic test automatically stops whenever the measured force amplitude exceeds the setting by 20%.

3. Fatigue results analysis

3.1 Shear force and relative tangential displacement

This section will focus on the evolution in applied shear force and its correspondence with the force control setting, in addition to the evolution in relative tangential displacement measured during the test.

For each cycle, both the force and displacement values were recorded at a 500-Hz frequency. A total of fifty points were thus used to plot each cycle. Fig. 7 shows the first five cycles of the applied shear force and measured relative displacement.

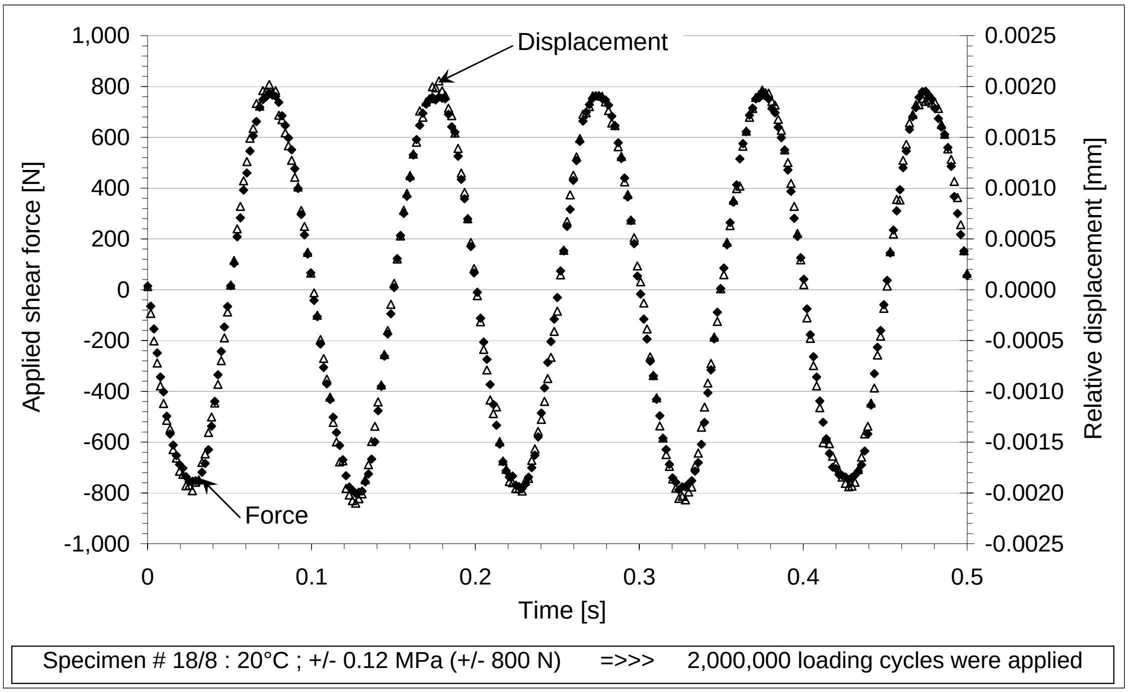

Fig. 7. First five cycles (applied force and resulting displacement) of the test

In addition to cycle accuracy (Fig. 7), the evolution in force and displacement amplitudes throughout the test is shown in Fig. 8, which indicates that the applied shear force amplitude matches the settings. Moreover, during the entire test, each force cycle is symmetric and alternating since the mean force value remains equal to zero.

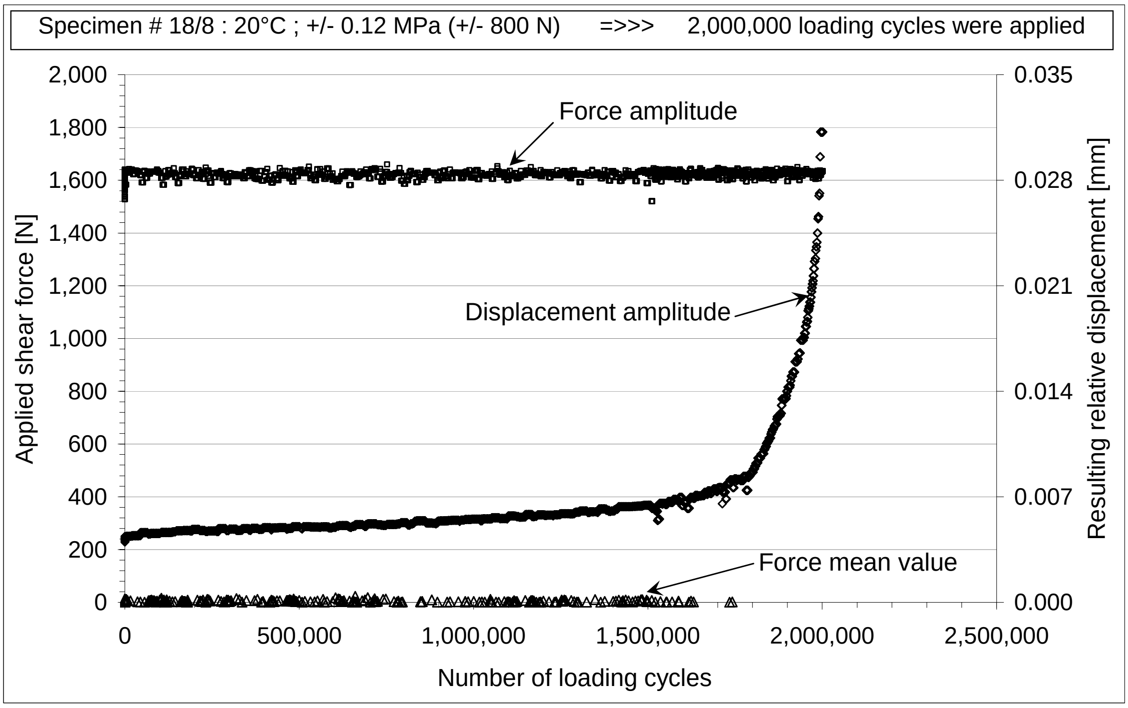

Fig. 8. Force and displacement amplitudes during the test

In focusing on the specimen failure mode, Fig. 9 displays a series of representative photographs, on which failure is clearly located at both interfaces. When a specimen is subjected to a high shear force (i.e. the oligocyclic test), macroscopic interface failure is sometimes accompanied by the aggregate interlock phenomenon.

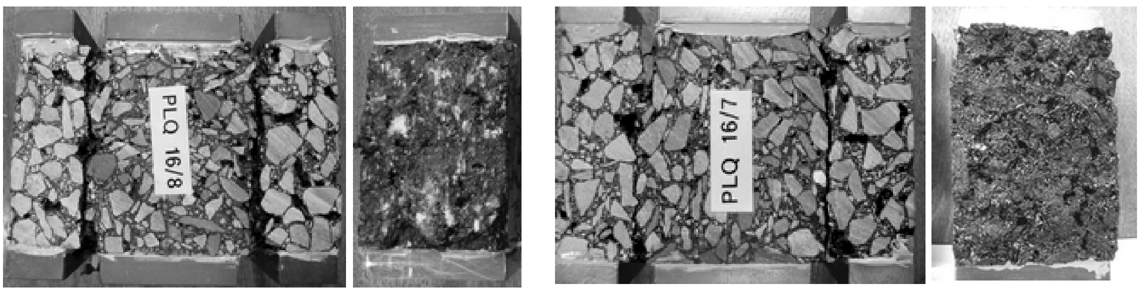

Oligocyclic test at 10°C, 10 Hz (20 loading cycles) | Aggregates interlock | Fatigue test at 10°C, 10 Hz (130,000 loading cycles) | Bitumen film at the interface

Fig. 9. Types of interface failure, depending on the force amplitude

3.2 Interface shear stiffness properties

The mechanical behaviour of the interface between two asphalt concrete layers is characterised by assessing the interface shear stiffness properties. This parameter correlates the applied shear stress with the resulting relative tangential displacement at the interface.

For each fatigue test, interface shear stiffness can be expressed as a complex number $K^*_{s,k}$, as described in Eq. (1):

$$\begin{cases} K^*_{s,k}(i\omega) = \dfrac{\Delta F_k}{S \cdot \Delta u_k} \cdot e^{i\varphi_k t} \\ \Delta K_{s,k} = \left| K^*_{s,k}(i\omega) \right| = \dfrac{\Delta F_k}{S \cdot \Delta u_k} \end{cases} \tag{1}$$

with (at cycle #k):

- $\Delta K_{S,k}$: the interface shear stiffness modulus
- ΔF_k: the applied shear force amplitude
- Δu_k: amplitude of the measured relative displacement
- φ_k: phase angle between the shear force and relative displacement signals
- S: sheared cross-sections of both interfaces;
- $\Delta\tau = \Delta\tau_k = \dfrac{\Delta F_k}{S}$: amplitude of the applied shear stress

Let's now turn our attention to the evolution in interface shear stiffness modulus (ΔK_S) during the fatigue test. As a result representative of fatigue testing, the normalised values of this stiffness modulus will be plotted against the number of loading cycles (Fig. 10). This trend curve can be divided into two main stages. At first, the slow decrease may be tied to damage extension (appearance of microcracking). During the second stage, the interface shear stiffness modulus decreases quickly, which implies both the coalescence and rapid propagation of macroscopic cracks at the interface.

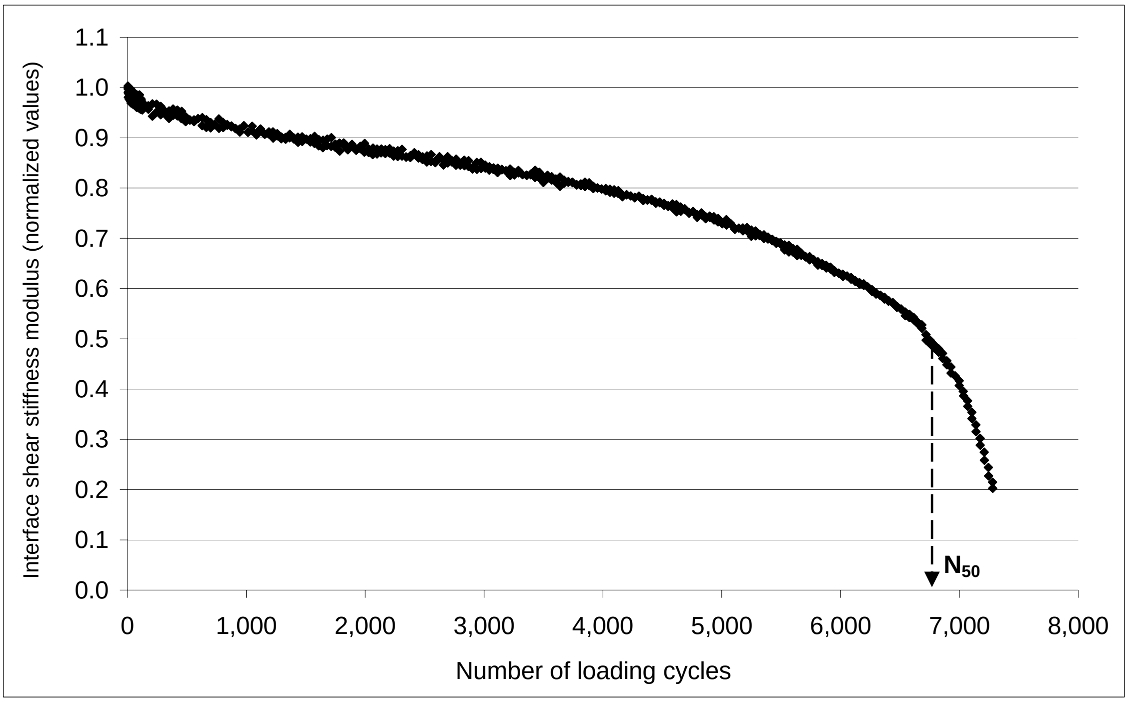

Fig. 10. Interface shear stiffness modulus vs. number of loading cycles

To further this analysis of fatigue test results, the relationship between applied shear stress amplitude and the resulting initial value of the interface shear stiffness modulus ($\Delta K_{S,1}$) needs to be investigated. The effects of both testing temperature and type of interface on this relationship also undergo a thorough analysis (Fig. 11).

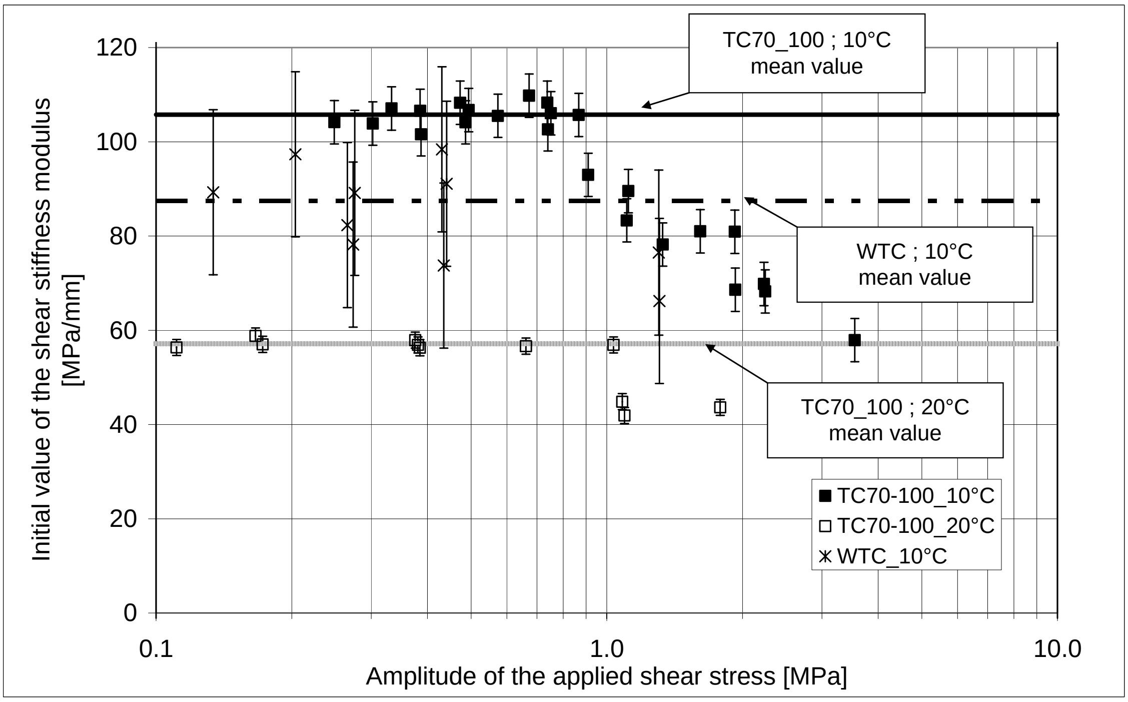

Fig. 11. Initial value of interface shear stiffness modulus vs. applied shear stress

Initial analysis of the results presented in Fig. 11 offers the following findings:

- The initial value of the interface shear stiffness modulus decreases as testing temperature rises for the same tack coat specimen;
- Upon first inspection, the absence of a tack coat leads to a smaller initial value of the interface shear stiffness modulus. This finding however is distorted by the scattering of results obtained for the interface without a tack coat (WTC case).

When this analysis is limited to results derived in the case of an interface with a tack coat, two types of behaviour can be clearly distinguished:

- When the applied shear stress amplitude is less than approx. 1 MPa, the initial value of the interface shear stiffness modulus is not affected by the loading amplitude; hence, the interface displays a linear viscoelastic behaviour;

- When the applied shear stress amplitude exceeds this roughly 1 MPa threshold, then the interface displays nonlinear behaviour. Moreover, in this study, a loading amplitude of greater than 1 MPa is typically applied when performing an oligocyclic test.

In the following sections, N_{50} (Fig. 10) will denote the number of loading cycles required to decrease by one-half the initial value of the interface shear stiffness modulus ($\Delta K_{S,1}$).

3.3 Viscoelastic properties

Since the number of measurement points (50) is sufficient to accurately plot each signal cycle (whether force or displacement), the formula in Eq. (2) is proposed to describe the relationship between force (or displacement) values and testing time.

$$\begin{cases} F_k(t) = \Delta F_k \cdot \sin\left(\omega \cdot t + \varphi_{Fk}\right) \\ u_k(t) = \Delta u_k \cdot \sin\left(\omega \cdot t + \varphi_{uk}\right) \\ \varphi_k = \varphi_{Fk} - \varphi_{uk} \end{cases} \quad (2)$$

At cycle #k, φ_k represents the phase angle between the force signal and the displacement signal. Throughout the test, the evolution in phase angle value is plotted against the normalised number of loading cycles (compared with N_{50}). From Fig. 12, it is observed that each phase angle evolution curve can be divided into three stages. During the first stage, the phase angle value increases quickly, perhaps as a result of a heat release process that tends to appear during the initial test cycles. The second stage then corresponds to a slowly increasing phase angle, turning into a very quickly increasing phase angle during the third stage. As expected, the phase angle value at

20°C is greater than that at 10°C, given that bituminous materials are more viscoelastic at higher temperatures.

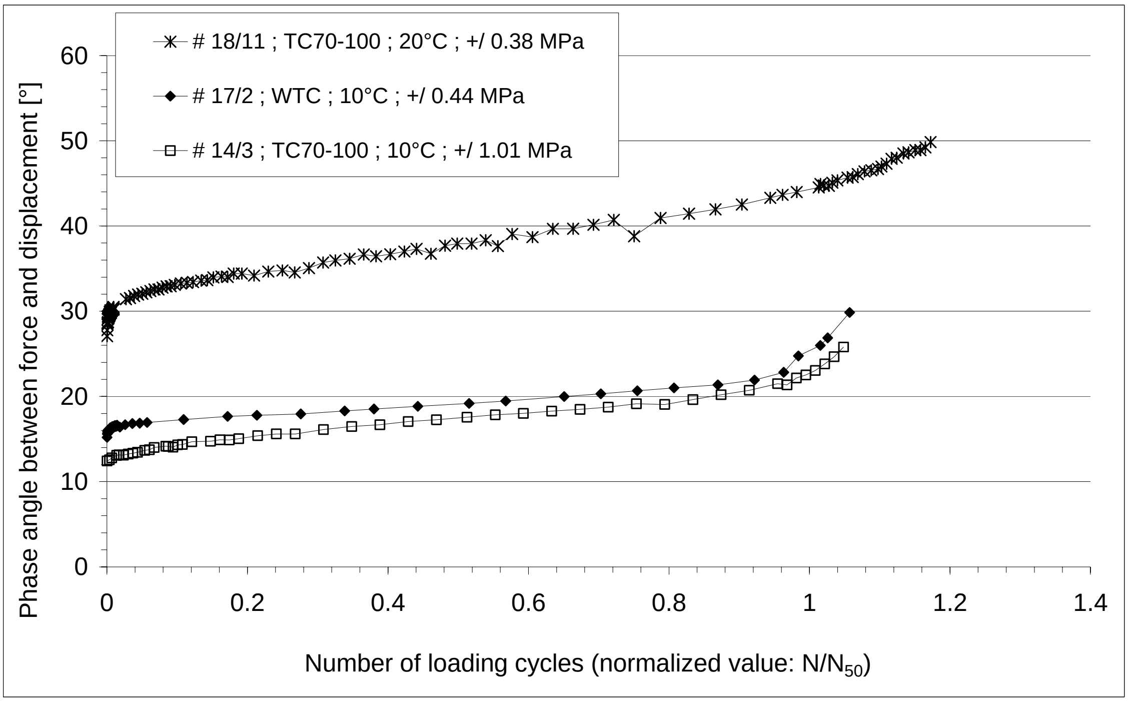

Fig. 12. Phase angle evolution during the test

It must now be known whether or not phase angle values provide information on the viscoelastic properties of the binder at the interface or on the asphalt concrete mix properties.

Ashayer [16] performed bending tests on asphalt concrete mixes at 10 Hz and 10°C. With a controlled force, the phase angle values he obtained were similar to those plotted in Fig. 12. Moreover, through a literature review [6,17], Mohammad *et al.* conducted dynamic shear rheometer tests in order to characterise the viscoelastic properties of various asphalt tack coats by measuring the properties of complex shear moduli and binder phase angles. The angles measured at 10°C, 25°C and 55°C equalled 55°, 65° and 70°, respectively. Based on these results, it can be concluded that the phase angle values obtained in our study describe an asphalt concrete behaviour, as opposed to a binder behaviour. This finding has been confirmed since at 10°C (Fig. 12), phase angle values appear to be low, whether influenced or not by the presence of a tack coat.

3.4 Interface fatigue performance

To take into account the effect of interface performance on pavement structure response, the pavement design engineer requires a fatigue law that correlates applied shear stress with the number of loading cycles to failure, which can obviously be determined by means of a failure criterion.

When referring to fatigue tests performed on asphalt concrete mixes, this failure criterion, which is related to the number of loading cycles to failure, is conventionally defined as a 50% decrease in the initial value of the elastic modulus ($|E^*|$).

In this section, the effects of both the tack coat and temperature on interface fatigue performance will be analysed by comparing the corresponding fatigue laws derived using the conventional failure criterion (i.e. a 50% drop in the $\Delta K_{S,1}$ value).

For each type of interface, studied at 10° as well as 20°C, the resulting fatigue laws with their 95% prediction intervals are presented in Fig. 13, which yields the following novel finding: results from both the oligocyclic and fatigue tests are highly correlated through a power law.

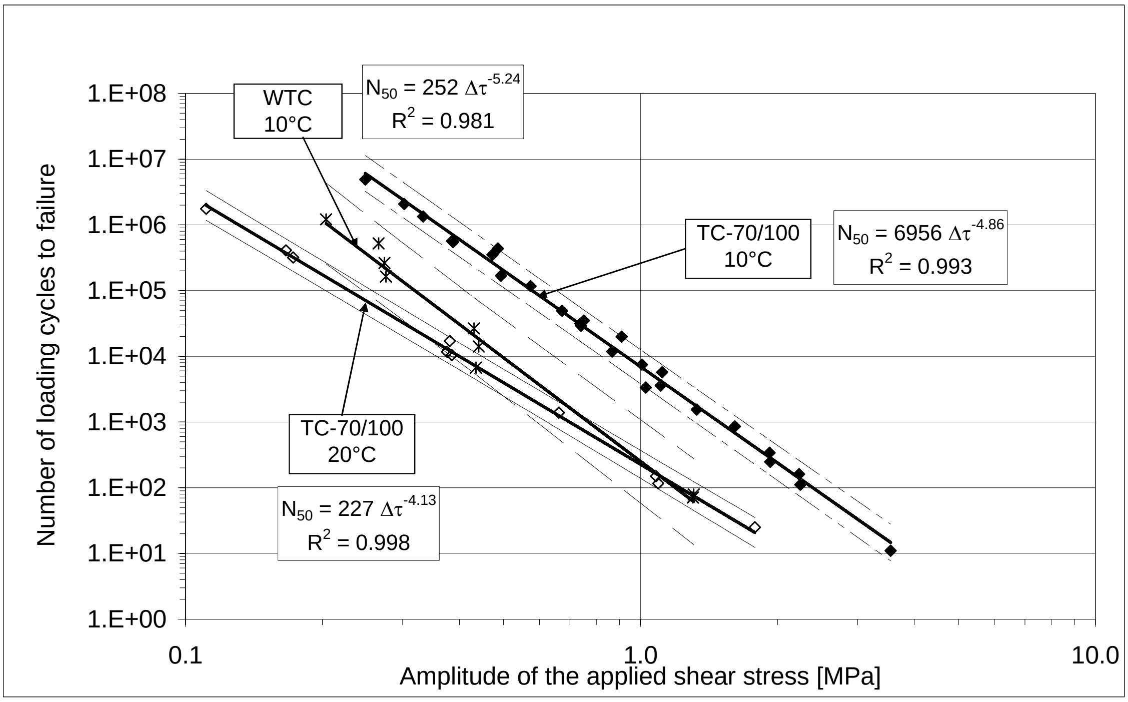

Fig. 13. Effect of interface conditions on bonding fatigue performance

At 10°C, it is clearly apparent that the lack of a tack coat leads to a strong decrease in the number of loading cycles to failure, hence a decline in interface fatigue performance as well. This constitutes a novel finding in that during monotonic shear tests, a number of results reveal only little effect on interface shear strength due to the lack of a tack coat [18]. At 10°C, fatigue results demonstrate the importance of applying a tack coat between asphalt concrete layers in enhancing the fatigue performance of bonding. Another finding from these fatigue results is the fact that at 10°C, the fatigue law slope seems to be unaffected by the type of interface (i.e. whether with or without a tack coat). It can thus be assumed that at 10°C, the fatigue law slope equals approx. -5.

In the case of an interface with a tack coat (i.e. TC-70/100), the two power laws proposed to describe interface fatigue behaviour at 10° and 20°C are indeed similar.

3.5 Determining interface fatigue parameters with shorter tests?

The interface failure criterion is based on a decrease in initial value of the interface shear stiffness modulus ($\Delta K_{S,1}$). As an example, the interface shear fatigue law will be analysed for each decrease by x% (from 10% to 70%) in the value of $\Delta K_{S,1}$ (Fig. 14).

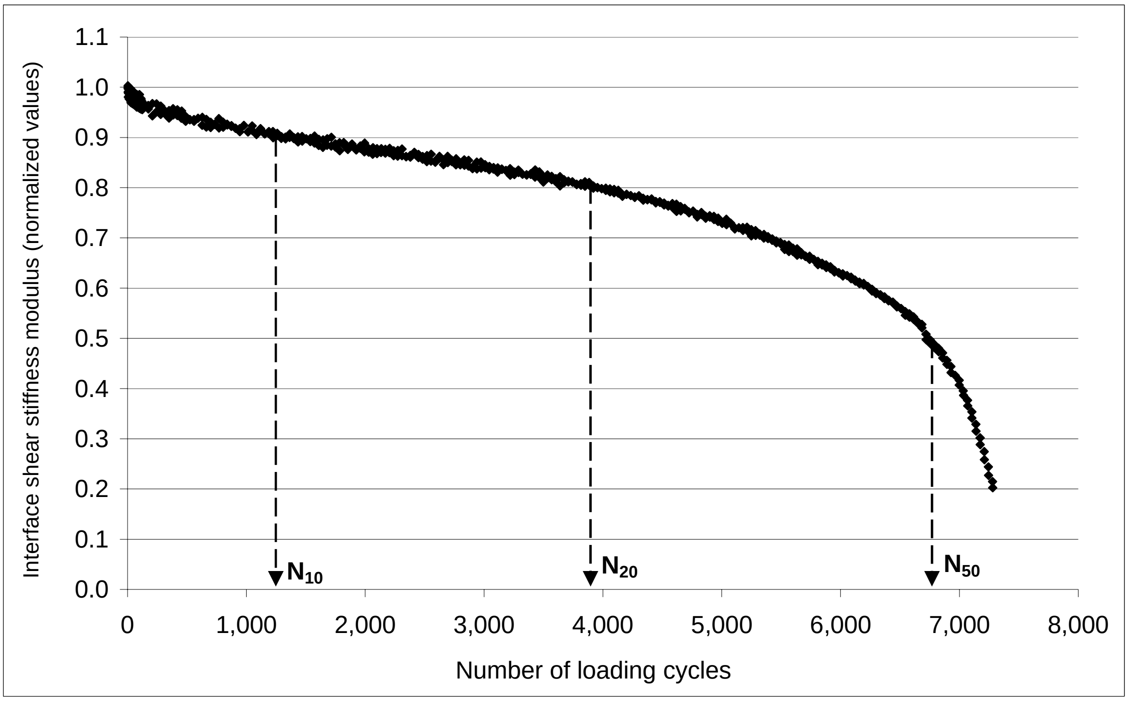

Fig. 14. Number of loading cycles corresponding to a drop in the value of $\Delta K_{S,1}$

On a log-log scale, for each drop in percentage (x) of $\Delta K_{S,1}$, the applied shear stress amplitude is plotted against the corresponding number of loading cycles to failure, N_x (Fig. 15). From this figure and for both oligocyclic and fatigue tests, a very good correlation can be observed between these two parameters (amplitude and N_x). This correlation is even better (i.e. less scattering of results) however when considering a percentage decline of more than 10. Otherwise, Fig. 15 reveals that for percentage decreases above 50, the shear fatigue laws obtained are nearly similar, due to the fact that fatigue tests are performed under force control. The interface quickly fails and the corresponding numbers of loading cycles to failure are practically equal.

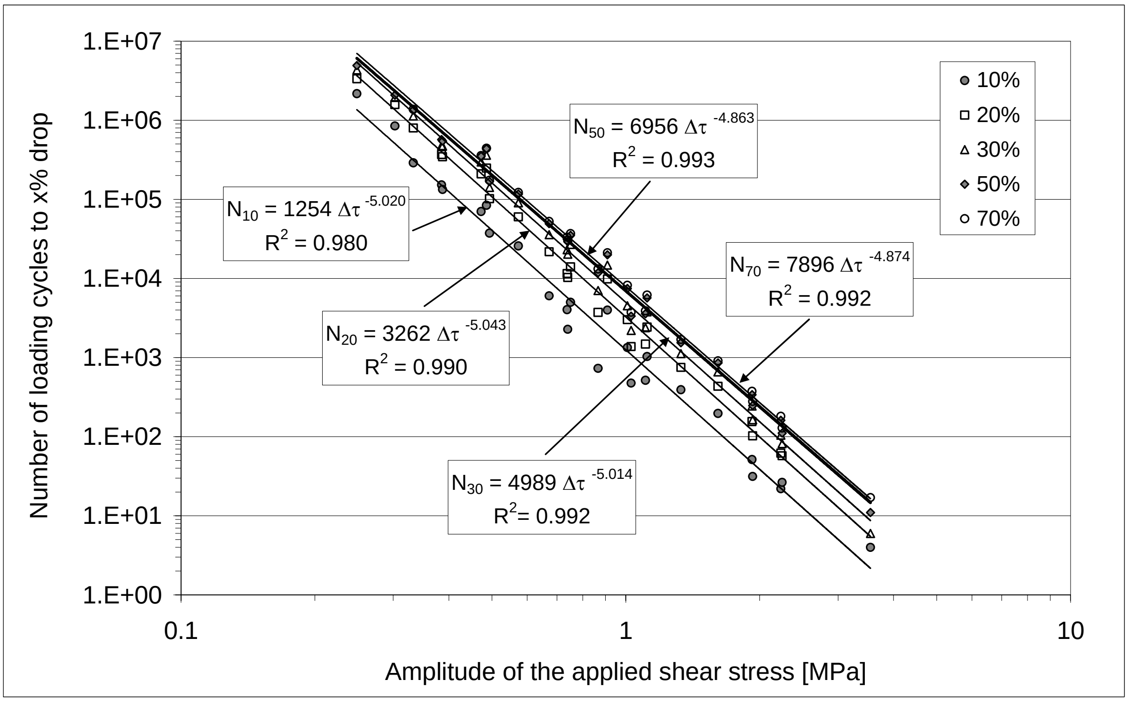

Fig. 15. Proposed interface fatigue law according to the fatigue criterion (TC 70-100)

In reference to the last finding, the interface failure criterion chosen to assess the number of loading cycles to failure is defined as a 50% decrease in the initial value of the interface shear stiffness modulus.

One well-known fact is that fatigue tests are time-consuming. The focus now turns to predicting the conventional fatigue law (i.e. a 50% drop in the value of $\Delta K_{S,1}$) on the basis of knowing the law with a drop of x% in $\Delta K_{S,1}$. For instance, several fatigue tests are performed before a 30% drop in $\Delta K_{S,1}$ can be achieved, at which point testing is stopped and a fatigue law derived from this failure criterion. Next, a prediction of the fatigue law corresponding to a 50% decrease in $\Delta K_{S,1}$ can be attempted.

From Fig. 15, we can then write the following equation (3):

$$\Delta\tau = A_x . N_x^{-b_x}$$

$$\log(N_x) = A_x - B_x \log(\Delta\tau) \text{ or } N_x = 10^{A_x} \cdot \Delta\tau^{-B_x} \quad (3)$$

The data analysis leads to identifying the various values A_x, B_x; Fig. 16 shows how these parameters evolve.

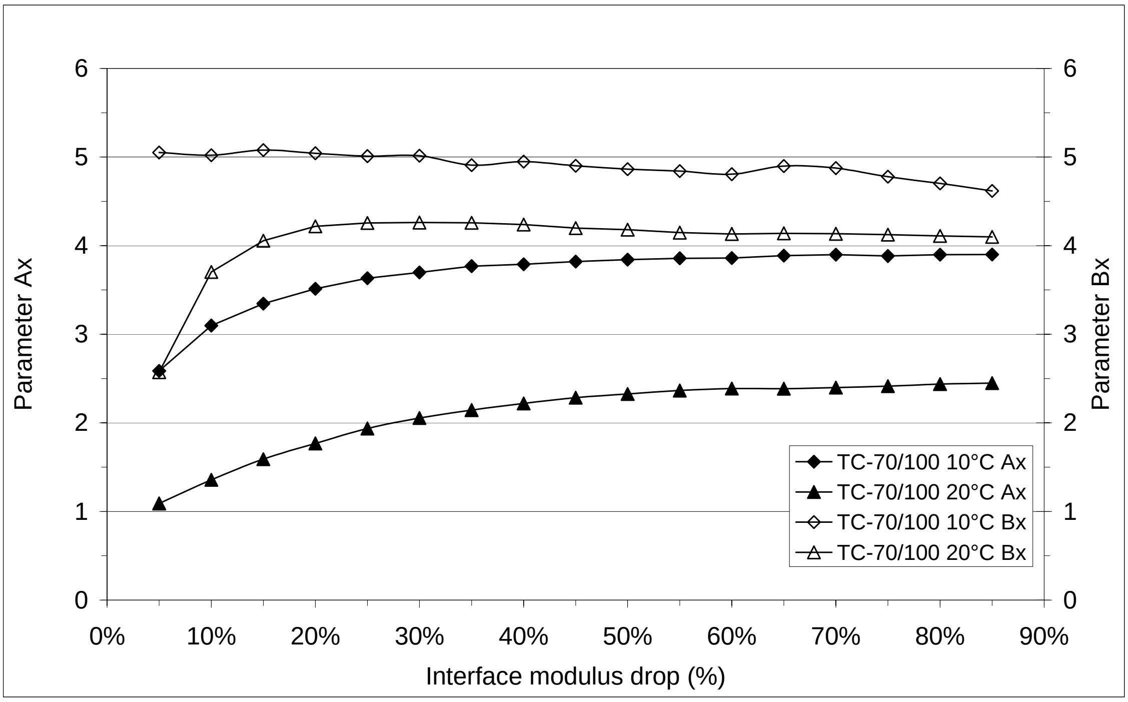

Fig. 16. Evolution of parameters A_x and b_x

Given Fig. 16, we now propose setting $B_x \cong B_{30} =$ constant for $x \geq 30$, while assuming the ability to stop fatigue testing once a 30% modulus drop has been achieved, so as to obtain a power-independent *x* (for $x > 30$). Moreover, for A_x to fit the experimental values, Eq. (4) can be introduced:

$$A_x = \frac{\alpha . x}{\beta + x} \quad (4)$$

For TC 70-100 at 10°C, the values $\alpha = 4.10$ and $\beta = 0.033$ can be identified, which yields $A_{50} = 3.845$; and $B_{50} = B_{30} \cong -5.01$; at this point, the model from Equations (3) and (4) offers:

$$N_{50} = 10^{A_{50}} \cdot \Delta\tau^{-B_{50}} = 7007 \cdot \Delta\tau^{-5.01} \qquad (5)$$

Both of the previous expressions calculate the standard parameter change when tests are stopped after a 30% modulus drop.

For this example, Fig. 15 produces the fatigue parameter from a complete test:

$$N_{50} = 6956 \cdot \Delta\tau^{-4.86} \qquad (6)$$

From Fig. 17, it is observed that fatigue laws extrapolated by shortened tests are in good agreement with these obtained by complete tests.

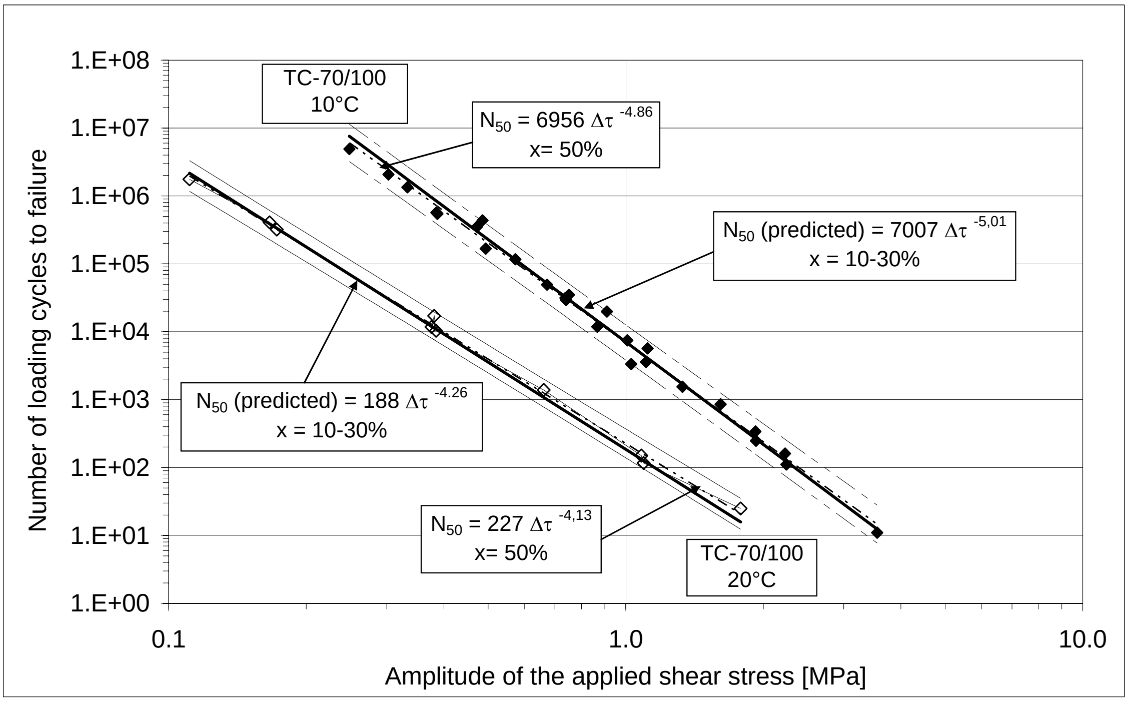

Fig. 17. Fatigue laws: short tests predictions vs. conventional fatigue tests (TC 70-100)

Table 2 shows a comparison of values of the amplitude of shear stress for the conventional life time $N_{50} = 10^6$ loading cycles, for shortened and complete tests on TC70/100. It can be seen from this table that relative errors on these values are less than

5% when tests are halted at 30% damage for the standard fatigue parameter identification.

Table 2. Amplitude of shear stress: shortened tests extrapolations vs. conventional fatigue tests (TC 70-100)

$\Delta\tau$ [MPa] for $N_{50} = 10^6$	TC 70-100 ; 10°C	TC 70-100 ; 20°C
complete test	0.360	0.131
predicted, x = 10-30%	0.372	0.133
relative error	3.3%	1.8%

In analysing the standard deviation (SD) from a bi-logarithmic diagram with a 5% risk, an SD value of 0.13 is found for TC 70-100 at 10°C and SD = 0.23 for an interface without a tack coat (WTC). In all cases, the SD value is less than that output from a conventional fatigue test (i.e. for a Hot Mix Asphalt (HMA) trapezoidal fatigue test at 10°C, SD = 0.3).

This method is beneficial for its high number of cycles, e.g. if $N_{50} = 10^6$ cycles, the test can be stopped at $N_{30} \approx 6 \cdot 10^5$ cycles, meaning that a fatigue test could last roughly 15-16 hours instead of nearly 30 hours, thus shortening test duration by around 50%.

4. Interface lifetime assessment using tack coat fatigue performance

This section is devoted to developing a model that enables the pavement engineer to incorporate both the interface lifetime and the lifetime of materials used in the pavement design process. The aim is to propose a model similar to the fatigue cracking model applied in France so as to assess the asphalt concrete layer lifetime. The notation $N_{50} = N$ has been adopted here since it reflects the conventional lifetime in pavement design.

The French fatigue cracking model [19] has been derived from bending tests performed on asphalt concrete specimens mixed in the laboratory at 10°C and 25 Hz. This model assumes the following form (Eq. (7)).

$$\varepsilon_t = \varepsilon_6 \cdot \left(\frac{N}{10^6}\right)^b \tag{7}$$

with:

- ε_t : amplitude of the applied tensile strain
- N : resulting number of loading cycles to failure
- ε_6 : applied tensile strain leading to failure after 1 million loading cycles
- b : slope of the fatigue law (by convention set equal to -0.20).

Similar to the fatigue cracking model, the interface fatigue model can be written as follows (Eq. (8)):

$$\begin{cases} \Delta\tau = \tau_6 \cdot \left(\frac{N}{10^6}\right)^b \\ \text{TC - 70/100}: \begin{cases} \text{At } 10°\text{C}, 10\text{ Hz}: \tau_6 = 0.36\text{ MPa}, b = -0.20 = -\frac{1}{B_{50}} \\ \text{At } 20°\text{C}, 10\text{ Hz}: \tau_6 = 0.13\text{ MPa}, b = -0.24 = -\frac{1}{B_{50}} \end{cases} \end{cases} \tag{8}$$

with:

- $\Delta\tau$: amplitude of the applied shear stress

- N : resulting number of loading cycles to failure

- $\Delta\tau_6$: applied shear stress leading to failure after 1 million loading cycles

- b : slope of the interface fatigue law.

The interface fatigue model (Eq. (8)) is used in the finite element program Cast3M to analyse the effect of incorporating interface fatigue performance in the pavement structure response, particularly for curved road sections. The numerical results [20] of this study have recently been published in the Road Materials and Pavement Design journal.

5. Conclusion

This paper has evaluated the bonding fatigue performance between two asphalt concrete (AC) layers. Such an innovative study represents one of the very first investigations of interface shear fatigue behaviour. The targeted interface lies between two AC layers, one very thin the other thick. Two interface conditions were investigated herein: with and without an asphalt tack coat.

For purposes of the experimental campaign, a customised double shear testing device was designed and built. The double shear test involves a specimen consisting of three AC layers bonded two-by-two. According to this configuration, both specimen interfaces are subjected to a relatively pure shear stress [14].

Oligocyclic as well as fatigue tests were carried out under force control at a frequency of 10 Hz with two temperatures (10° and 20°C). In this study, an analysis of fatigue results has mainly been based on the evolution in interface shear stiffness modulus, which correlates applied shear stress with the resulting relative tangential displacement. Several failure criteria have been analysed in order to derive the interface shear fatigue law. On a log-log scale, the applied shear stress amplitude was plotted against the number of loading cycles to failure. Results from both the oligocyclic and fatigue tests show very low scatter. In addition, at each testing temperature, a power law leads to a very good correlation between applied shear stress and number of loading cycles to failure. This finding is a very valuable one since the results of the fatigue and oligocyclic tests can now be plotted on the same diagram and correlated through a power law. Another novel finding from this study is that at 10°C, the lack of tack coat leads to a decrease in bonding fatigue performance, which means that at this temperature, applying a tack coat improves interface fatigue shear performance.

At 10°C, the interface fatigue law slope appears not to be influenced by the type of interface (i.e. with or without a tack coat). This slope is -0.20, i.e. the same as that obtained from fatigue tests carried out on asphalt concrete mixtures. Based on results found in the case of an interface with a tack coat, the interface fatigue law slope equals approximately -0.24 at 20°C.

The fact that fatigue tests are time-consuming comes as no surprise. To overcome this constraint, it has been sought to predict the conventional interface fatigue law from more accelerated fatigue tests. The conventional failure criterion is defined as a 50% decline in initial value of the interface shear stiffness modulus ($\Delta K_{S,1}$). A method was proposed to allow predicting the conventional fatigue law from tests halted once an x% drop (with x being less than 50) in $\Delta K_{S,1}$ has been achieved. A very small deviation exists between the predicted conventional fatigue law and the "true" law.

Beyond these fatigue results, a fatigue model has been taken forward to assess the interface lifetime. The interface fatigue model is expressed on the basis of the model currently used to determine the lifetime of asphalt concrete mixtures. A recently published paper has focused on use of the interface fatigue model to improve the design of curved road sections [20].

6. References

[1] Raab C, Partl MN. Interlayer bonding of binder, base and sub-base layers of asphalt pavements: long term performance. Constr and Build Mater 2009; 23(8): 2926-2931.

[2] Collop AC, Sutanto MH, Airey GD, Elliot AC. Shear bond strength between asphalt layers for prepared samples and field cores. Constr and Build Mater 2009; 23(6): 2251-2258.

[3] Romanoschi SA, Metcalf JB. Characterization of asphalt concrete layer interfaces. Transportation Research Record 2001; 1778: 132-139.

[4] Romanoschi SA, Characterization of pavement layer interfaces, Ph.D. Thesis, Louisiana State University, Baton Rouge, 1999, 152 p.

[5] Canestrari F, Ferrotti G, Partl MN, Santagata E. Advanced testing and characterization of interlayer shear resistance. Proceedings of the 84th TRB annual meeting, 2005, 26 p.

[6] Mohammad LN, Wu Z, Raqib MA. Investigation of the behavior of asphalt tack coat interlayer. Louisiana Transportation Research Centre 2005; Project N° FHWA/L.A. 04/394, 126 p.

[7] Miro-Recasens R, Martinez A, Perez-Jimenez F. Assessing heat-adhesive emulsions for tack coat. Proceedings of the Institution of Civil Engineers transport

2005; 158(1): 45-51.

[8] Partl MN, Canestrari F, Ferrotti G, Santagata FA. Influence of contact surface roughness on interlayer shear resistance. Proceedings of the 10th International Conference on asphalt pavement 2006; Quebec.

[9] Diakhaté M, Phelipot-Mardelé A, Millien A, Petit C. Shear fatigue behaviour of tack coats in pavements. Road Mater and Pavement Design 2006; 7(2): 201-222.

[10] Chaignon F, Roffe J-C. Characterisation tests on bond coats: worldwide study, impact, tests, recommendations. International Bitumen Emulsion Federation (IBEF) 2001; 9: 12-19.

[11] Al-Hakim B, Cheung LW, Armitage RJ. Use of FWD data for prediction of bonding between pavement layers. International Journal of Pavement Engineering 2000; 1(1): 49-59.

[12] Raab C, Partl MN, Abd El Halim AO. Evaluation of interlayer shear bond devices for asphalt pavements. Baltic Journal of Road and Bridge Engineering 2009; 4(4):176-195.

[13] Ascher D, Wellner F. *Untersuchungen zur Wirksamkeit des Haftverbundes und dessen Auswirkungen auf die Lebensdauer von Asphaltbefestigungen.* [Investigation of the effectiveness of bonding and its influence on the service life of asphalt pavements]. Technical University of Dresden, Germany, 2007; Report No. 13589 BR/1: 100 p.

[14] Diakhaté M, Fatigue et comportement des couches d'accrochage dans les structures de chaussée, Ph.D. Thesis, Université de Limoges, France, 2007.

[15] Petit C, Laveissière D, Millien A. Modelling of reflective cracking in

pavements: fatigue under shear stresses. Proceedings of the 3rd International Symposium on 3D FE for Pavement Analysis, Design and Research: Amsterdam, 2002, p. 111-123.

[16] Ashayer SMA, Comportement en fatigue des enrobés bitumineux. Ph.D. Thesis, INSA de Lyon, France, 1998.

[17] Lesueur D, La rhéologie des bitumes: principes et modification. *Rhéologie* 2002; 2 : 1-30.

[18] Mrawira D. Revisiting the effectiveness of tack coats in HMA overlays: the shear strength of tack coats in young overlays. Proceedings of the 14th TRB annual conference 1999; 1616: 116-129.

[19] LCPC-SETRA. Conception et dimensionnement des structures de chaussée, guide technique. Paris, 1994.

[20] Petit C, Diakhaté M, Millien A, Phelipot-Mardelé A, Pouteau B. Pavement design for curved road sections: fatigue performance of interfaces and longitudinal top-down cracking in multilayered pavements. Road Mater and Pavement Design 2009; 10(3): 609-624.

7. Figure captions

Fig. 6. Fatigue testing equipment

Fig. 7. First five cycles (applied force and resulting displacement) of the test

Fig. 8. Force and displacement amplitudes during the test

Fig. 9. Types of interface failure, depending on the force amplitude

Fig. 10. Interface shear stiffness modulus vs. number of loading cycles

Fig. 11. Initial value of interface shear stiffness modulus vs. applied shear stress (the error bars represent the 95^{th} percentile confidence limits)

Fig. 12. Phase angle evolution during the test

Fig. 13. Effect of interface conditions on bonding fatigue performance

Fig. 14. Number of loading cycles corresponding to a drop in the value of $\Delta K_{S,1}$

Fig. 15. Proposed interface fatigue law according to the fatigue criterion (TC 70-100)

Fig. 16. Evolution of parameters A_x and B_x (TC 70-100)

Fig. 17. Fatigue laws: short tests predictions vs. conventional fatigue tests (TC 70-100)

8. Table captions

Table 1. Design characteristics of the tested asphalt concrete (AC) mixes

Table 2. Amplitude of shear stress: shortened tests extrapolations vs. conventional fatigue tests (TC 70-100)